Selectivity Effects on Series Reactions by Reactant Storage and PSA Operation

Adriaan J. Kodde, Ymke S. Fokma, and Alfred Bliek
Dept. of Chemical Engineering, University of Amsterdam, NL-1018 Amsterdam, The Netherlands

This work evaluates adsorptive reactors used to improve the operation of a sequential reaction scheme, $A \xrightarrow{+D} B \xrightarrow{+D} C$, for the total removal of A from a stream with an excess of B. In the adsorptive-reactor concept, the reactor is filled with a physical mixture of catalyst and an adsorbent, the latter being thermodynamically selective toward primary reactant A. In this case, the sorbent is periodically regenerated using the principles of pressure swing adsorption and purged with secondary reactant D. This concept is restricted to low temperatures to have sufficient adsorption capacity. Improved reaction selectivity arises from the accumulation of A in the unit. The reaction of A maximizes the driving force for regeneration and thus accelerates the regeneration half-cycle. The adsorptive reactor is compared to a conventional plug-flow reactor (PFR) and to PSA and PFR units in series. Reaction selectivity improved and pure B recovered over these alternative reactors under realistic conditions. The volume-based productivity is lower than that of PFR, but higher than that of PSA. The purge-gas flow rate can be manipulated to balance the sorption flux and reaction rate, thereby maximizing the conversion of A. The influence of differences in sorption kinetics is discussed and the required sorbent characteristics are identified.

Introduction

Pressure-swing adsorption (PSA) is an established separation technology based on selective, reversible adsorption of one or more components in a gas mixture onto an adsorbent (Ruthven, 1984; Ruthven et al., 1994; Yang, 1987). Selective adsorption can either be based on differences in sorption equilibria or on different sorption kinetics. PSA operation consists of alternating adsorption and regeneration steps, and the unit is run in a cyclic invariant state. The design of such units is not straightforward due to the large number of operating parameters and its intrinsic dynamic character. Although a few rules of thumb are known, detailed simulation is essential for design (LaCava et al., 1998).

Vaporciyan and Kadlec (1987) were the first to extend PSA to chemical reactors, thereby employing *in-situ* separation of products/reactants during chemical conversion. They proposed to use a mixture of a catalyst and a sorbent in the reactor vessel and operate it under a pressure-swing cycle. Such a reactor is now known as the pressure-swing reactor (PSR), pressure-swing adsorber reactor (PSAR), sorption-enhanced reaction process (SERP), or adsorptive reactor. The *in-situ* separation can be used to improve the performance of a chemical reactor. Several operating principles can be utilized.

Equilibrium-limited reactions can be driven to completion by separation of the reaction products. The use of PSR in connection with equilibrium-limited reactions has been investigated over the past several years. Besides numerous parametric studies, application to a number of processes has been evaluated, including the water–gas shift reaction for H_2 production by CO_2 adsorption (Han and Harrison, 1994), water–gas shift reaction for CO production by H_2O adsorption (Carvill et al., 1996; Anand et al., 1996), steam–methane reformation for H_2 production by CO_2 adsorption (Hufton et al., 1999), cyclohexane dehydrogenation by H_2 storage (Goto et al., 1993), methyl-cyclohexane dehydrogenation by toluene adsorption (Yongsunthon and Alpay, 1999), and NH_3

Correspondence concerning this article should be addressed to A. Bliek or A. J. Kodde.
Present address of Y. S. Fokma: The Boston Consulting Group, JF Kennedylaan 100, 3741 EH Baarn, The Netherlands.

synthesis (Kneabel and Cussler, 1996). An overview of early work in this field was given by Carvill et al. (1996).

In contrast to equilibrium-limited reversible reactions, irreversible reactions have received little attention in PSR research and the focus has been on rate improvement. Alpay studied the reaction $A \rightarrow B$ in a rapid PSR, where the adsorption affinity of A dictates the residence time in the vessel and thus conversion (Alpay, 1992). Vaporciyan and Kadlec (1989) showed that the rate of CO oxidation can be increased by adsorbing CO, since the reaction rate is inversely proportional to the CO partial pressure.

In the present work we focus on sequential irreversible reactions, where selectivity toward reaction intermediates is the crucial parameter. An example is the selective hydrogenation of acetylenes (Derrien, 1986). In previous work we have shown that by selectively adsorbing the reaction intermediate B in a sequential reaction scheme: $A \rightarrow B \rightarrow C$, selectivities beyond those obtained in a steady-state-operated plug-flow reactor can be obtained under pressure-swing operation (Kodde and Bliek, 1997). This result was later confirmed by Sheikh et al. (1998) for a CSTR.

In the sequential irreversible reaction scheme: $A \xrightarrow{+D} B \xrightarrow{+D} C$, where selectivity toward B is the crucial parameter, separation of B and D by selectively adsorbing B can also increase the selectivity toward this product. The soundness of this principle was illustrated for batch operation in a chromatographic reactor (Liden and Wamling, 1989).

In case of a feed mixture with both A and B present, application of the preceding principle has some pitfalls. Component B from the feed can saturate the sorbent and minimize the operating capacity of the sorbent.

For such systems we propose to enhance the selectivity toward B by reactant storage. When feeding a mixture of A and B, A will accumulate in the reactor vessel by adsorption onto the sorbent, and is thus not available for reaction; A will be absent before the adsorption front. These conditions are unfavorable for operation as the availability of the desired reactant A is reduced. We therefore propose to start the reaction as the adsorption front of A reaches the product end and reactant D is introduced as purge gas in the regeneration step. At this moment the ratio of A over B present in the vessel is much more favorable than the feed-gas composition, resulting in improved reaction selectivities over an ordinary PFR. Secondly, the conversion of A by reaction will further lower its gas-phase concentration, and thus maximize the driving force for regeneration and improve the productivity of the unit. With the proposed operation, separation and reaction are integrated in space, but separated in time.

In this work we address the question of whether this operating principle can be put to work in a PSR unit and employed to yield improved performance over traditional reactor configurations.

Reactor Models

Three reactor configurations are compared in this work: (1) a PSR reactor where equal volumes of catalyst and adsorbent are perfectly mixed; (2) a PFR with an identical amount of catalyst as in (1), (3) a PSA with the sorbent followed by a PFR with the catalyst. The stream enriched in A from the PSA is sent to the PFR.

A reactor model was derived using the following assumptions:

1. Isothermal operation;
2. Ideal gas law is obeyed;
3. Axially dispersed plug flow in the bed;
4. Negligible pressure drop over the bed;
5. Adsorbent and catalyst of constant voidage, bulk density, and particle size;
6. No radial concentration gradients;
7. Perfect mixing of the catalyst and adsorbent particles;
8. Adsorption isotherm of the Langmuir type;
9. Mass-transfer resistance is described by the linear driving-force model;
10. Reactions are first order in reactant partial pressures,
11. The specific time constant for catalytic reactions is negligible to that of other processes in the reactor.

Isothermicity clearly is the most stringent assumption and will be relaxed in future work.

For parametric studies, it is convenient to write the governing equations in their corresponding dimensionless form. The adsorption step (P_{high}, v(prod)) and PSR reactor length (L) are used as a reference state. The resulting variables and parameters are given in the notation section. The single-species mass balance reads:

Model*

	Pres.		Ads		Depres.		Purge	
	$x=0$	$x=1$	$x=0$	$x=1$	$x=0$	$x=1$	$x=0$	$x=1$
y	(a)		(a)		(b)		(c)	
V	Eq. 2	$V=0$	Eq. 2	$V=1$	Eq. 2	$V=0$	Eq. 2	$V=-\psi$
P	$\frac{\partial P}{\partial \tau}=\Upsilon_{pres}$		$P=1$		$\frac{\partial P}{\partial \tau}=\Upsilon_{depres}$		$P=\Omega$	
	$x=0$				$x=1$			
(a)	$\frac{\partial}{\partial x}(y_i)=PeV[y-y_i(\text{feed})]$				$\frac{\partial}{\partial x}(y_i)=0$			
(b)	$\frac{\partial}{\partial x}(y_i)=0$				$\frac{\partial}{\partial x}(y_i)=0$			
(c)	$\frac{\partial}{\partial x}(y_i)=0$				$\frac{\partial}{\partial x}(y_i)=PeV[y-y_i\,(\text{purge})]$			

*See Figure 1.

$$\frac{\partial}{\partial \tau}(y_i P) = -P\frac{\partial}{\partial x}(V y_i) + \frac{P}{Pe}\frac{\partial^2}{\partial x^2}(y_i) - \chi_i^a \frac{\partial}{\partial \tau}(\theta_i) + \nu_{i,1} R_1 + \nu_{i,2} R_2 \qquad i = 1 \cdots N. \quad (1)$$

The overall mass balance reads:

$$\frac{\partial}{\partial \tau}(P) = -P\frac{\partial}{\partial x}(V) - \Sigma_i \chi_i^a \frac{\partial}{\partial \tau}(\theta_i) + \Sigma_i \nu_{i,1} R_1 + \Sigma_i \nu_{i,2} R_2. \quad (2)$$

Sorption kinetics using the linear driving-force model:

$$\frac{\partial}{\partial \tau}(\theta_i) = \Phi_i(\theta_i^* - \theta_i) \qquad i = 1 \cdots N. \quad (3)$$

The sorption equilibrium using the Langmuir isotherm:

$$\theta_i^* = \frac{\kappa_i y_i P}{1 + \kappa_i y_i P} \qquad i = 1 \cdots N. \quad (4)$$

The reaction rates:

$$R_1 = K_1 y_A y_D P^2 \quad (5)$$

$$R_2 = K_2 y_B y_D P^2. \quad (6)$$

The boundary conditions are given in Table 1. The PFR model is the steady-state equivalent of the PSR model at the adsorption stage. The PSA model is identical to the PSR model without the reaction terms.

The PSA and PSR units in this study are operated in the single-bed version of the four step Skarstrom cycle (Karstrom, 1960) (Figure 1). For the PSA, part of the product gas is temporarily stored in a well-mixed tank. During pressurization/depressurization a constant-pressure ramp rate was assumed. The gas-flow velocities at the product end of the bed were fixed.

The PFR model is the steady-state equivalent of the PSR in the adsorption step with no adsorbent present and half the reactor length. The PSA model is equivalent to the PSR model with no catalyst present and half the reactor length.

The performance indicators used for all units are the conversion of A (X_A), the reaction selectivity (R_1/R_2), and the productivity (Pr). Productivity is based on the amount of feed gas processed per second and multiplied by the reference state

$$\left[\frac{\epsilon^g v(\text{prod}) P_{\text{high}}}{\epsilon^{a/c} \rho^{a/c} LRT}\right]$$

has units of $\text{mol}_{\text{feed}} \cdot \text{s}^{-1} \cdot \text{kg}_{\text{ads}}^{-1}$ for the PSA and PSR and $\text{mol}_{\text{feed}} \cdot \text{s}^{-1} \cdot \text{kg}_{\text{cat}}^{-1}$ for the PFR unit. Further performance indicators are the product stream purity of A over A, B, and C (Pu_A), and the recovery of B (Rv_B). The definitions of these indicators are given below.

The cumulative flux of a component in a stream is defined as an auxiliary variable:

$$J_i(\text{stream}) = \int_{\tau_{\text{cycle}}} \pm y_i V_{x=0 \wedge x=1} P \, d\tau, \quad (7)$$

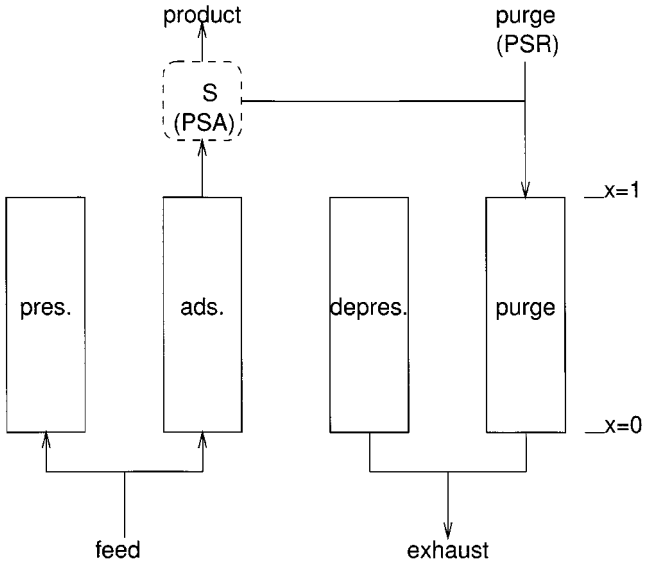

Figure 1. Skarstrom cycle for pressure swing operation.

For the PSA, S represents an ideally mixed storage tank where part of its contents is used as purge gas at low pressure. For the PSR, component D is introduced via the purge feed at low pressure.

where the cycle time is given by $\tau_{\text{cycle}} = \tau_{\text{pres}} + \tau_{\text{ads}} + \tau_{\text{depres}} + \tau_{\text{purge}}$. The net consumption of a component over one cycle is given by

$$\Delta J_i = J_i(\text{feed}) - J_i(\text{prod}) + J_i(\text{purge}) - J_i(\text{exh}). \quad (8)$$

The performance indicators defined in terms of J and ΔJ are:

$$X_A = \frac{\Delta J_A}{J_A(\text{feed})} \quad (9)$$

$$R_1/R_2 = \frac{\Delta J_A}{\Delta J_C} = \frac{\int_{\tau_{\text{cycle}}} \int_0^1 K_1 y_A y_D P \, dx \, d\tau}{\int_{\tau_{\text{cycle}}} \int_0^1 K_2 y_B y_D P \, dx \, d\tau} \quad (10)$$

$$Pr(\text{PSA}) = \frac{\Sigma_{i=A,B} J_i(\text{feed})}{\tau_{\text{cycle}}} \quad (11)$$

$$Pr(\text{PFR}) = \sum_{i=A,B} V_{x=0} y_{i,}(\text{feed}) P \quad (12)$$

$$Pu_A(\text{prod}) = \frac{J_A(\text{prod})}{\Sigma_{i=A,B,C} J_i(\text{prod})} \quad (13)$$

$$Rv_B(\text{prod}) = \frac{J_B(\text{prod})}{J_B(\text{feed})} \quad (14)$$

$$Pu_A(\text{exh}) = \frac{J_A(\text{exh})}{\Sigma_{i=A,B,C} J_i(\text{exh})} \quad (15)$$

$$Rv_B(\text{exh}) = \frac{J_B(\text{exh})}{J_B(\text{feed})}. \quad (16)$$

The inventory of species i in the vessel is given by

$$A_i = \int_0^1 \left(\chi_i^a \theta_i + y_i P \right) dx. \qquad (17)$$

The initial state is a vessel completely filled with reactant D. The relaxation to cyclic steady state is calculated by successive integration. Convergence to the cyclic steady state is assumed on the basis of the following balances:

$$\Delta J_A + \Delta J_B + \Delta J_C = 0$$
$$\Delta J_A + \Delta J_C - \Delta J_D = 0.$$

The first expression represents a check on the conservation of the main reactant/product and the second is a check on the consumption of auxiliary reactant D. Convergence was assumed when the residues equaled the integration accuracy (10^{-8}).

Numerical Solution of the Model

The model was implemented in *gPROMS* Version 1.6 (Process Systems Enterprise Ltd., London, U.K.). Discretization of the axial domain was implemented using a second-order upwind scheme (Gaskell and Lau, 1988, Table 1) on a staggered grid. The upwind scheme proved more suitable for this model for problems with flow reversal than the built-in schemes (central finite differencing or orthogonal collocation). The staggered grid is preferred since the boundary conditions of the balances are expressed in terms of fluxes. The axial reactor axis was discretized using 200 equal volumes. An IBM RS6000 43P workstation and a Pentium III PC were used in the simulations.

Model Parameters

The objective of the unit is to remove all A from the feed stream, which consists of 10% A in B, and obtain high recovery of B. To enable a proper comparison the allowed impurity level of A in the product stream is fixed at 5 ppm for each case. The adsorption step is terminated when the preset purity of the product stream is reached. Likewise, the regeneration time is coupled to the extent of regeneration (PSR) or to the amount of product stream gas (PSA).

The parameters are given in Table 2 and discussed below. The Peclet number in industrial adsorbers is usually high. Reaction occurs in a PSR when A or B and D are both present in the gas phase. During pressurization and adsorption this situation only occurs at the unretended front, and thus the extent of reaction depends strongly on the Peclet number. In reality the reaction zone may be broader due to the finite residence time of the species on the catalytic surface. Therefore a relatively small Peclet number of 200 was chosen for the PSR system. This Peclet number still gives rise to mass transfer, predominantly by convection, and requires a reasonable number of grid points using nondedicated algorithms. The Peclet number for the PFR and PSA system are derived using the same value for the axial dispersion coefficient (D_{ax}).

Table 2. Parameter in the Simulations

	PSR Cases			PSA Cases		PFR Cases	
Symbol	I	II	III	IV	V	VI	VII
$\chi^a_{A\ldots D}$	20	20	20	40	40		
Φ_A	0.5	0.5	0.5	0.5	0.5		
$\Phi_{B\ldots D}$	0.5	0.5	5	0.5	5		
κ_A	10	10	10	10	10		
κ_B	2	2	2	2	2		
κ_C	1	1	1	1	1		
κ_D	0	0	0	0	0		
K_1	2,000	20,000	2,000			2,000	20,000
K_2	200	2000	200			200	2,000
P_e	200	200	200	50	50	100	100
Ω	1/3	1/3	1/3	1/3	1/3		
Υ_{pres}	1/30	1/30	1/30	1/6	1/6		
Υ_{depres}	$-9\ 1/3$	$-9\ 1/3$	$-9\ 1/3$	$-1/6$	$-1/6$		
τ_{ads}	*	*	*	*	*		
τ_{purge}	**	**	**	†	†		
y_A (feed)	0.1	0.1	0.1	0.1	0.1	0.05	0.05
y_B (feed)	0.9	0.1	0.1	0.9	0.9	0.45	0.45
y_C (feed)	0.0	0.0	0.0			0.00	0.00
y_D (feed)	0.0	0.0	0.0			0.50	0.50
y_A (purge)	0.0	0.0	0.0	Pu_A(prod)	Pu_A(prod)		
y_B (purge)	0.0	0.0	0.0	Pu_B(prod)	Pu_B(prod)		
y_C (purge)	0.0	0.0	0.0				
y_D (purge)	1.0	1.0	1.0				
ψ	††	‡	††	2‡‡	2	Variable	Variable

*The step is terminated when the following criterion is met: $Pu_A(\text{prod}) > 5 \times 10^{-6}$.
**The step is terminated when the following criterion is met: $A_A < 10^{-3}$.
†The step is terminated when the following criterion is met: $\Sigma J(\text{purge})/\Sigma J\ (\text{prod}) = 0.7$.
††Values used: 0.5, 1, 2, 5, 10, 20, 50, 100.
‡Values used: 1, 2, 5, 10, 20, 50, 100, 200, 500, 1,000.
‡‡Optimal value; see Figure 2.

In Table 3 the sorbent properties selected for the present case are compared to values used in experimentally verified simulations of equilibrium-based PSA systems. The values for saturation capacity (χ_i^a) and adsorption kinetics (Φ_i) used in the base case are within the range of experimental values reported in the literature. The resulting retention factor

$$\left\{ \frac{\chi_A \theta_A^* \left[y(\text{feed}), P_{\text{high}} \right]}{y_A(\text{feed})} \right\}$$

is comparatively high, but much higher values (*n*C6 on zeolite 5A) have been reported. The resulting sorption selectivity chosen in the base case is very modest compared to the PSA systems.

The reaction selectivity ratio (k_1/k_2) of the catalyst was fixed at 10. Since the molar ratio of *A* to *B* in the feed is set at 9, a net conversion of *B* already becomes apparent at low conversion levels.

In the PSA and PFR in the series case, the purpose of the PSA unit is to purify the feed stream and optimize the *A*-to-*B* ratio in the exhaust stream. The purge gas velocity was chosen at its optimal value ($\psi = 2$), as both the recovery of *B* in the product stream [Rv_B(prod)] and the enrichment of *A* in the exhaust stream [Pu_A(exh)] reside at their local maxima (Figure 2).

To keep realistic gas-flow velocities in the pressurization step, the pressurization rate (Υ_{pres}) is set to a low value. The depressurization rate (Υ_{depres}) is fast to minimize initial slip of *A*.

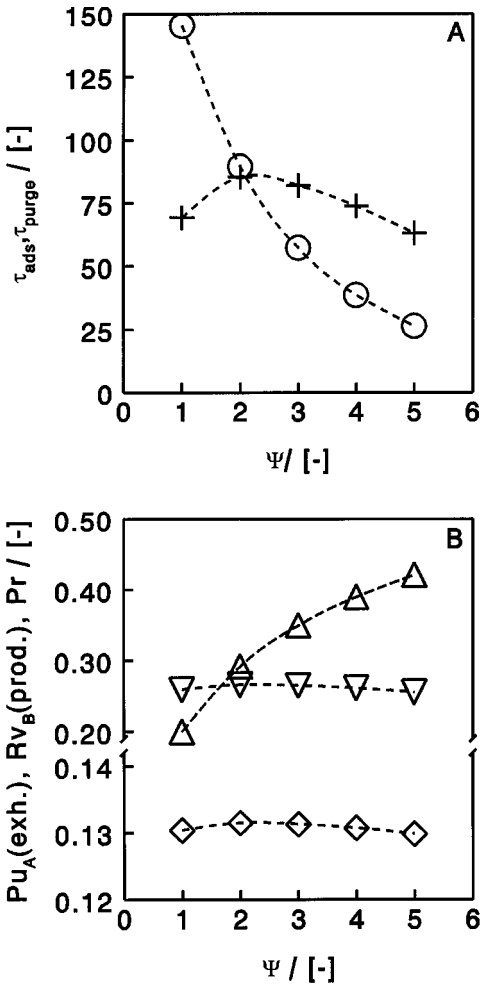

Figure 2. Influence of purge gas flow rate (ψ) on PSA performance.

+: τ_{ads}; ○: τ_{purge}; Δ: *Pr*; ▽: Rv_B(prod); ◇: Pu_A(exh). Parameters: PSA case IV in Table 2.

Results

Reactor performance: recovery, selectivity, and productivity

The overall performance of the PSR is compared to the PSA and PFR in series and the PFR in Figures 3, 4, and 5, which show the recovery of *B*, reaction selectivity, and productivity, respectively.

In Figure 3 the three configurations are compared as separators by plotting purity vs. recovery. For the PSR, *A* is removed by adsorption and over 80% of *B* is recovered at high purity in the high-pressure half-cycle. This combination of recovery and purity cannot be obtained in a PFR. The recovery

Table 3. Comparison of Key Adsorption Parameters with Selected PSA Systems

	PSA in This Work	Farooq et al., 1989 (Exp. No. 8)	Yang et al., 1997 (Run C′)	Yang et al., 1997 (Run C)	Silva and Rodriques, 1998 (PSA Case)
A		O_2	CH_4	CO	nC_5/nC_6
B		N_2	H_2	H_2	*i*C5
Sorbent		Zeolite 5A	Zeolite 5A	Zeolite 5A	Zeolite 5A
y_A (feed)	0.1	0.21	0.3	0.3	0.139/0.046
y_B (feed)	0.9	0.79	0.7	0.7	0.815
χ_A^a	40	44.96	12.65	13.39	99.35
χ_B^a	40	44.96	6.72	6.72	0
Φ_A	0.5	28.7	0.17	0.08	*
Φ_B	0.5	9.1	2.10	2.11	*
$\frac{\chi_A \theta_A(y(\text{feed}), P_{\text{high}})}{y_A(\text{feed})}$	200	5.74	18.11	25.61	73/800
$\frac{\chi_B \theta_B(y(\text{feed}), P_{\text{high}})}{y_B(\text{feed})}$	28.58	18.1	0.59	0.44	0
Ω	0.333	0.230	0.091	0.091	0.133

* Variable.

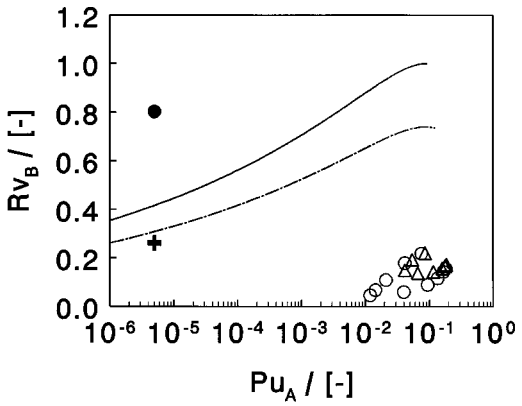

Figure 3. Purity of *A* vs. recovery for various reactor configurations.

Dotted line: PFR case VI,VII;+: PSA and PFR case IV prod. stream; continuous line: PSA and PFR case IV exh. stream; ●: PSA case I and II prod. stream; Δ: PSR case I exh. stream; ○: PSR case II exh. stream. Parameters: see Table 2.

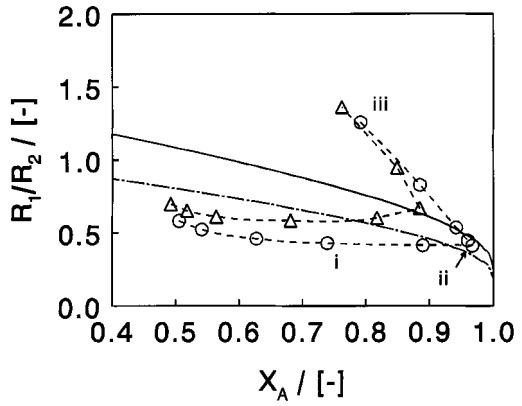

Figure 4. Reaction selectivity vs. conversion of *A*.

Dotted line: PFR case VI,VII; continuous line: PSA and PFR case IV; Δ: PSR, case I; ○: PSR case II. Parameters: see Table 2. The numbers correspond to the cases shown in Figure 6.

of *B* in the product stream of the PSA unit is much lower, as part of this gas is used as purge gas. Due to the selective adsorption, *A* is accumulating in the PSR, and the ratio of *A* and *B* present in the vessel (A_A/A_B, see Eq. 17) rises from 0.111 to 0.57 during the adsorption step.

Figure 4 compares the three configurations as reactors by comparing conversion with reaction selectivity. In the PSR the reaction takes place almost exclusively in the regeneration step. At the onset of pressurization, the vessel is filled with *D*. The feed velocity during pressurization is dominated by the net consumption of moles during reaction at the concentration front of *B* until all *D* is converted. Since *A* is retarded, it is hardly converted at this stage. The regeneration behavior can be manipulated both by the catalyst activity and the residence time of the reactants. The residence time of the reactants is directly related to the purge-gas velocity. High conversions can only be obtained when both parameters are large compared to the desorption rate of *A* and *B* (see

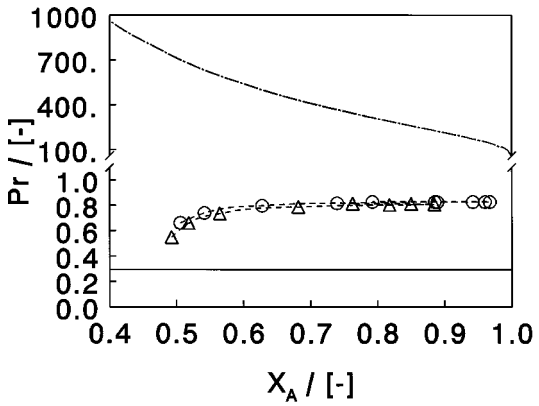

Figure 5. Productivity vs. conversion of *A* for different reactor configurations.

Dotted line: PFR case VI; Δ: PSR case I; ○: PSR case II; continuous line PSA case IV. Parameters: see Table 2. For PFR case VII the productivity is ten times the value for the PFR case VI shown here.

Figure 4). For high purge-gas flow rates the PSR demonstrates an overall selectivity to *B* far in excess of that observed for both the PFR and the PSA and PFR in series.

A second advantage of the PSR is that it leads to acceleration of the regeneration by conversion of the desorbed gas. The resulting shorter purge times and more thorough regeneration enhances the productivity of the unit. Figure 5 shows that this is indeed the case. The PSR has much higher productivity compared to the PSA. The required purge time hardly depends on purge gas velocity ($\tau_{\text{purge}} \approx 19.5$) and is close to the theoretical minimum

$$\tau_{\text{purge}} = \frac{1}{\Phi_A}^{e} \log\left(\frac{A_{A,\text{start}}}{A_{A,\text{end}}}\right) \approx 18$$

The productivity of the PSA unit is limiting in the PSA and PFR in series. Therefore its productivity is independent of conversion. The PFR has the highest productivity. In the PFR the molar fraction of *A* in the gas phase is on the order of a few percent, whereas it is usually below 0.1% during regeneration in the PSR. Compared to the PSA and PFR case, which is the traditional choice for maximizing selectivity, the PSR offers a productivity improvement by a factor of 3.

Optimal operation: balancing the sorption flux and reaction rate

A distinct optimum exists in conversion with respect to purge-gas velocity (Figure 4). This can be understood by the dynamics of the regeneration. Figure 6 shows qualitative differences in regeneration behavior for the three cases. In case I a significant initial outflow of unconverted *A* is observed until two-thirds of *A* is removed, followed by a period of regeneration without outflow of *A*. In the optimal case the outflow of *A* only occurs in the depressurization step. In the case of higher purge flows, the outgoing flux of unreacted *A* is constant in time. These three cases are illustrated in Figure 7.

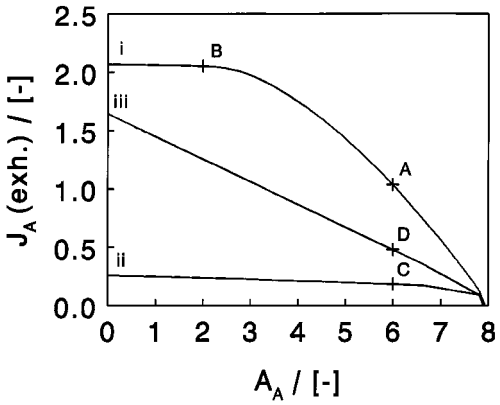

Figure 6. Outgoing flow of *A* during regeneration in a PSR.

i: $\psi = 10$; ii: $\psi = 50$; iii: $\psi = 1000$. Parameters: PSR case II (Table 2). The letters refer to the cases shown in Figure 7.

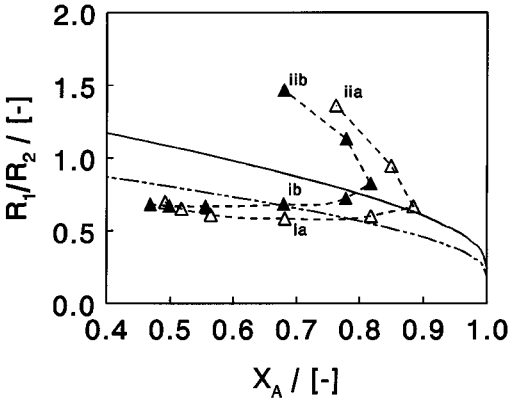

Figure 8. Influence of kinetic selectivity on reaction selectivity ratio (R_1/R_2) vs. conversion (X_A) for two PSR systems.

Dotted line: PFR case VI; continuous line: PSA and PFR case IV, V; Δ: PSR case I; ▲: PSR case III. For the PSA and PFR cases IV and V the two lines overlap in this graph. The numbers in the graph correspond to cases shown in Figure 9.

In the case where purge-gas velocity is too low, it takes a significant time for *D* to penetrate through the reactor. During this time, desorption of *A* is balanced by the reaction after this front *only* (Figure 7A). The outflow of *A* drops once *D* reaches the end of the vessel (Figure 7B).

The maximum conversion of *A* is reached when sorption and reaction are balanced throughout the regeneration. This case is shown in Figure 7C.

Upon a further increase in the purge-gas flow, the reaction rate can no longer balance the desorption flux. This results in significant outflow of *A* throughout the regeneration step (Figure 7D). Thus, optimum conversion can be reached by balancing the adsorption kinetics and the catalyst activity. The conversion of *A* is constrained by the amount of *A* released during depressurization and the molar fraction present in the gas phase at the end of the adsorption step.

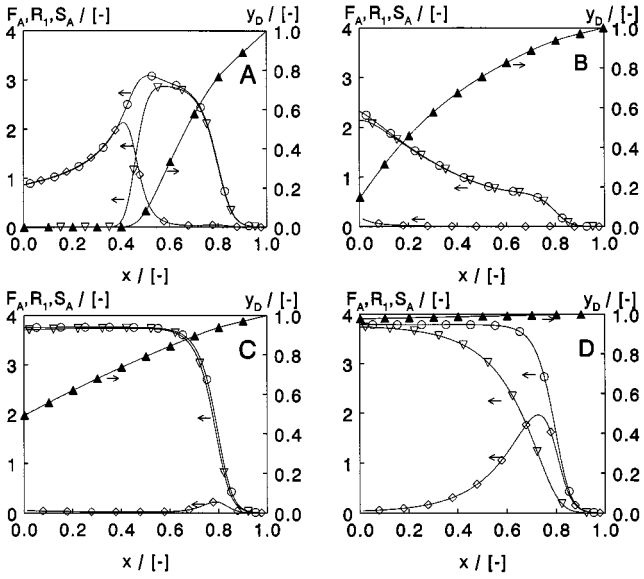

Figure 7. Profiles in the reactor during regeneration.

▲: y_D; ○: desorption flux of A (S_A); ▽: R_1; ◇: flow of A (F_A). Parameters: PSR case II: A, B; $\psi = 10$; C: $\psi = 50$; D: $\psi = 1000$. For each case the extent of regeneration is illustrated in Figure 6.

Combined thermodynamic and kinetic sorption selectivity

Since the sorption rate is a key parameter in PSR operation, kinetic selectivity can be exploited. Swift removal of adsorbed *B* may result in additional enhancement of the reaction selectivity. This was evaluated by a series of simulations where the sorption rates of *B* and *C* were increased tenfold that of *A*, resulting in a system that is thermodynamically selective toward *A* and kinetically selective toward *B* (PSR case III in Table 2).

Figure 8 shows that the selectivity improvement is small compared to the nonkinetic case (PSR case I). A slight improvement at low purge velocities is found, but the conversion of *A* is lower. Compared to the base case the ability of the sorbent to separate *A* and *B* is reduced, and hence the accumulation of *A* in the vessel by adsorption drops from $A_A = 8$ to around 6. This reduces the potential for selectivity enhancement. The underlying phenomena are discussed shortly. Upon depressurization the initial rise of y_A observed in the base case is absent due to the fast desorption of *B* (not shown). As a result the extent of reaction 1 ($A \xrightarrow{+D} B$) during the initial stage of the purge step is reduced. Later on *B* is nearly fully removed and the selectivity rises to end at slightly higher values. The latter two phenomena are illustrated in Figure 9, which shows that the initial drop in selectivity is reversed in the course of the regeneration.

Hence, the increased reaction selectivity during the major part of the regeneration cycle is largely counteracted by a reduced accumulation of *A* during the adsorption cycle and the unfavorable onset of the regeneration half-cycle.

As mentioned before, the inclusion of kinetic selectivity toward *B* reduces the ability of the sorbent to separate *A* and *B*. On a tenfold increase in catalyst activity compared to the kinetically selective case just treated (PSR case III, ▲ in Fig-

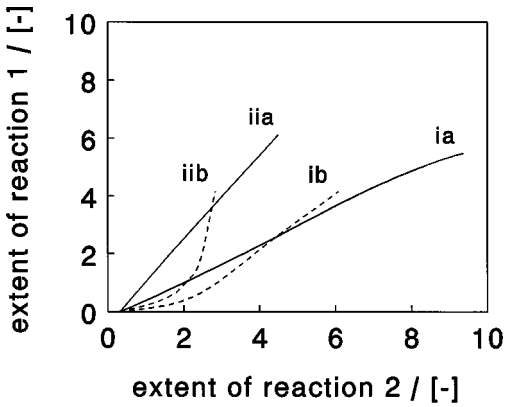

Figure 9. Development of the reaction selectivity during the regeneration for kinetically and nonkinetically selective cases.

Incremental reaction selectivity is given by the slope of the lines. The numbers are shown in Figure 8. Continuous lines and a: PSR case I (Figure 8: Δ); dotted lines and b: PSR case III (Figure 8: ▲); i: $\psi = 5$; ii: $\psi = 100$.

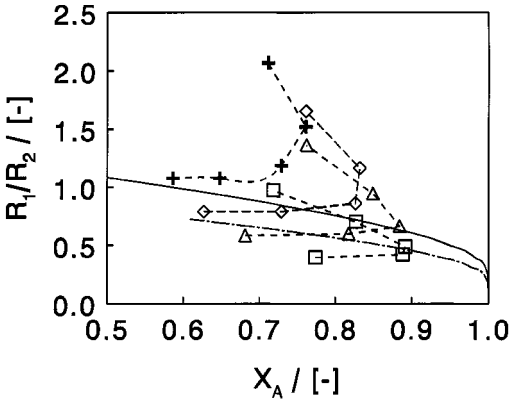

Figure 11. Influence of sorbent capacity on the performance of the PSR.

Dotted line: PFR case VI; continuous line: PSA and PFR case IV; PSR case I modified with □: $\chi^a_{A\ldots D} = 10$; Δ: $\chi^a_{A\ldots D} = 20$; ◇: $\chi^a_{A\ldots D} = 40$; +: $\chi^a_{A\ldots D} = 100$ (cases shown here: ψ = 5,10,20,50,100).

ure 8), the required purity of the product stream cannot be met. This is illustrated in Figure 10, which shows the resulting concentration profiles of component A (y_A) during pressurization in the cyclic steady state.

The in-going flow rate is comparatively high due to the high net consumption of moles. Due to differences in sorption kinetics, retention of B is now dominant and A accumulates at the interface with D. This results in molar gas fractions of A above the feed-gas composition. The high conversion rate of A (R_1) results in the swift penetration of A through the reactor while it simultaneously reacts. In the course of pressurization, the superficial gas velocity drops and now thermodynamics determine the relative retention of A over B. This results in a broad concentration front of A.

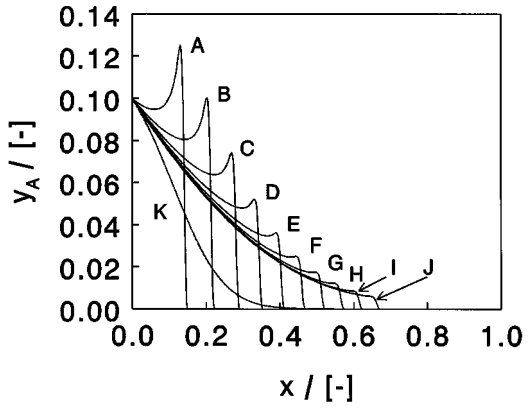

Figure 10. Profiles of the molar gas fraction of A (y_A) over the reactor during the pressurization step in case of combined kinetic and thermodynamic sorption selectivities.

A to J: The lines are plotted started at $\tau = 0.195$, with increments of 0.1 until $\tau = 1.095$. Parameters: PSR case III modified with $K_1 = K_1 \times 10$, $K_2 = K_2 \times 10$, $\psi = 2$. K: PSR case III; $\psi = 2$ after an identical total amount of feed gas was fed ($\tau = 3.5$).

At the reactor end, the concentration of A reaches a maximum of 300 ppm early in the pressurization process. Subsequently it drops to about 10 ppm at the start of the adsorption step, and then rises again. As a result, the purity limit of 5 ppm can never be met and the adsorption step is terminated right after its minimum step time ($\tau_{ads} = 1$).

Performance criteria for the sorbent

For the performance of the PSR, the ability of the sorbent to selectively retain A in the unit is of paramount importance. In this section, the minimum requirements for sorbents are addressed. Sorbent capacity and selectivity were systematically investigated by varying χ_i^a and κ_B, respectively.

An increase in the sorbent capacity leads to higher reaction selectivities, but it lowers the maximum attainable conversion (Figure 11). The retention ratio of A to B (A_A/A_B at $\tau = \tau_{ads}$) increases with increasing adsorbent capacity, which leads to higher reaction selectivities. The flux of desorbing species (S_A) is proportional to the saturation capacity (χ_A^a) and will also increase. As shown in the section on reactor performance a high conversion can only be obtained when both the purge flow velocity and catalyst activity are large compared to the desorption rate. This situation is no longer encountered for when the sorbent capacity increases and the sharp maximum in the conversion of A versus the purge-gas flow velocity disappears.

When the adsorption affinity of B becomes less, the reaction selectivity and the maximum attainable conversion of A in the PSR increase (Figure 12). The former is directly related to the decreased retention of B in the unit. The latter results from the decreased amount of D consumed in the conversion of B during the regeneration, which results in swifter penetration of D into the reactor.

There is no single generic criterion to determine which one of the investigated reactor configurations is optimal. The parameters of PSR case I represent the case where the reaction selectivity at the maximum conversion is just higher than the

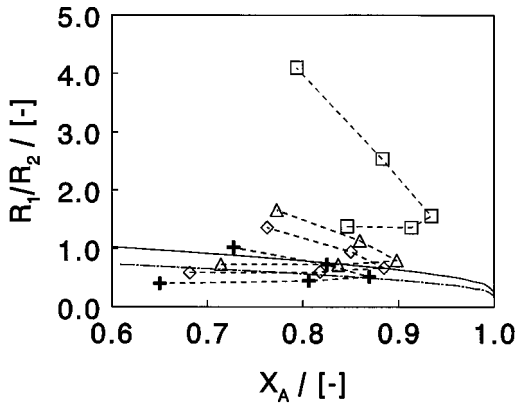

Figure 12. Influence of sorbent selectivity on the performance of the PSR.

Dotted line PFR case VI; continuous line PSA and PFR case IV; PSR case I modified with +: $\kappa_B = 5$; ◇: $\kappa_B = 2$; Δ: $\kappa_B = 1$; □: $\kappa_B = 0$ (cases shown here: ψ = 5,10,20,50,100).. Boundary Conditions for the Vessel

alternative reactor configurations (PSR case I, Δ: $\psi = 50$ in Figure 4). A sorbent with lower capacity or selectivity should be operated at a much higher purge velocity to obtain reaction selectivities beyond the alternative reactor configurations, and the resulting conversion drops sharply. The base case presented in this study reflects the case where the sorbent properties are only just appropriate to justify PSR operation.

In this work we assume the PSR contains equal volumes of catalyst and sorbent. For higher catalyst activities than assumed in this base case, the balancing reaction rate and sorption flux can be achieved by using less catalyst; thus the dilution of sorbent by catalyst particles decreases and the criterion on the sorbent with respect to its capacity (χ_i^a) can be relaxed to minimally approach half the value given here.

In the case of lower sorbent capacities ($\chi^a_{A\ldots D} = 10$) the required purity of the product stream could not be met in PSA and therefore the PSR data should be compared to the PFR only. In the PSR the purity of the product stream is reached as a result of the reaction, which induces a more thorough regeneration in the PSR concept.

Discussion

In the PSR a moderate pressure ratio in the pressure swing cycle is generally sufficient, as sorbent operation is largely driven by partial pressure reduction. This adds to the viability of the concept. A similar observation was made by Yongsunthon and Alpay (1998) in a study on temperature-swing adsorptive reactors. They found that optimal operation required a regeneration temperature *below* the adsorption temperature, as the desorption was largely driven by concentration swing.

The PSR concept is restricted to low temperatures and easy separation of *D* from *A*, *B*, and *C*. The former is required to meet the sorbent capacity requirement, and the latter to remove *D* from the product exhaust stream.

We have shown that the purge-gas flow rate can be used to balance the reaction rate and desorption kinetics. The sorbent-to-catalyst mixing ratio and temperature level can also be used to achieve this balance.

The Skarstrom cycle is usually applied in pressure-swing adsorption to obtain a pure product stream only. In this study a large recycle ratio was needed in order to meet the required purity. Also the resulting enrichment of *A* in the exhaust stream was limited to approximately 35%. There is a great deal of room for improvement in both the PSA and PSR in this study: a cocurrent depressurization step may be included to increase the fraction of *A* in the exhaust stream (Chen and Yang, 1986). Also for the PSR, variation of purge-gas flow velocity within the purge step can be used to tune the corresponding residence time of the reactants during regeneration. However, the use of more sophisticated pressure swing cycles is beyond the scope of this work.

The PSR concept can also be used to improve an existing PSA separation application. The inclusion of a catalyst will lead to a more thorough regeneration in a shorter regeneration time. Furthermore, systematic variation of the adsorption capacity has shown that due to a more thorough regeneration, the requirements on sorbent capacity for the required separation can be relaxed. Finally, a reactive purge gas will increase the recovery of the components in the product stream.

Selective hydrogenations represent a class of reactions where selectivity is crucial. Front-end acetylene hydrogenation is carried out industrially at 40°C and 25 bar (Derrien, 1986). We are currently studying the selective hydrogenation of acetylene as a model reaction for this system experimentally.

Conclusions

In this work we have addressed the use of a packed bed filled with a mixture of a sorbent and a catalyst, and operated in a pressure-swing mode. The PSR concept is compared to both a plug-flow reactor (PFR), a pressure-swing separation, and a plug-flow reactor in series (PFR and PSA). In the case presented here, the unit is used to carry out the reaction scheme $A \xrightarrow{+D} B \xrightarrow{+D} C$. The feed stream is a mixture of *A* and *B*, and the objective is to remove *A* from the feed by selective adsorption, and then to introduce reactant *D* to selectivity react *A* and *D* in the *B*-depleted reactor.

As a reactor, we have shown that the superior selectivity performance of the PSR concept was seen for realistic sorbent properties, and hence the PSR concept is viable in a practical sense for low-temperature reactions in particular.

As a separator, the inclusion of a catalyst will allow sorbent regeneration to be carried out in a time close to the theoretical minimum, which leads to a factor ≈ 3 improvement in the productivity compared to the PSA. The productivity is, however, lower compared to the single PFR unit.

A maximum conversion level in the PSR is obtained when the sorption kinetics and the reactor kinetics are balanced.

For the realistic parameters (PSR case I) in this study, the selectivity at maximum achievable conversion in the PSR is just higher than the PFR or PFR and PSA. These parameters limit the region where optimal conversion and a small selectivity improvement are combined. In the case of larger sorbent selectivities and higher sorbent capacities, the selectivity enhancement of the PSR increases at optimal conversion.

Acknowledgment

Academic Computing Services Amsterdam (SARA) is gratefully acknowledged for making available CPU time on their SP2 platform.

Notation

A_I = amount of component i inside the reactor, Eq. 17
b = adsorption affinity, Pa^{-1}
D_{ax} = axial dispersion coefficient, $m^2 \cdot s^{-1}$
F_A = axial flux of component A, $-(\partial V y_A/\partial x)+(P/Pe)(\partial^2 y_A/\partial x^2)$
$J_i(s)$ = cumulative flux of component i in stream s, Eq. 7
k = reaction rate constant, $mol \cdot kg^{c-1} \cdot s^{-1} \cdot Pa^{-2}$
K_j = amount catalyst and catalyst activity, $(\epsilon^c \rho^c k_j P_{high}^2 LRT)/[\epsilon^g P_{high} v(prod)]$
K_{LDF} = adsorption rate constant, s^{-1}
L = reactor length, m
P = pressure, Pa
P = dimensionless pressure, (P/P_{high})
Pe = axial dispersion coefficient, $[v(prod)L]/D_{ax}$
Pr = productivity, Eqs. 11, 12
$Pu_i(s)$ = purity of stream s with respect to component i, Eqs. 13, 15
q = solid phase concentration, $mol \cdot kg^{-1}$
R = gas constant, $J \cdot mol^{-1} \cdot K^{-1}$
$Rv_i(s)$ = recovery of component i in stream s, Eqs. 14, 16
R_1/R_2 = reaction selectivity, Eq. 10
S_A = desorption flux of component A, $-\chi_A^a(\partial\theta_A/\partial\tau)$
t = time, s
T = absolute temperature, K
v = superficial gas velocity, $m \cdot s^{-1}$
V = interstitial velocity, $v/v(prod)$
x = length, z/L
X_A = conversion of A, Eq. 9
y = molar gas fraction
z = axial distance from reactor feed, m
ϵ^j = volume fraction of phase j, $m_j^3 \cdot m_{total}^{-3}$
θ_i = amount adsorbed, q_i/q_i^{sat}
κ_i = adsorption equilibrium, $P_{high} b_i$
$\nu_{i,j}$ = stoichometric coefficient of component i in reactor j
ρ = mass density, $kg \cdot m^{-3}$
τ = time, $tv(prod)/L$
Υ_{depres} = depressurization rate, $[(P_{low}-P_{high})/P_{high}][L/v(prod)t_{depres}]$
Υ_{pres} = pressurization rate, $[(P_{high}-P_{low})/P_{high}][L/v(prod)t_{pres}]$
Φ_i = adsorption rate, $K_{LDF,i}L/v(prod)$
χ_i^a = amount adsorbent and capacity, $\epsilon^a \rho^a q_i^{sat} RT/\epsilon^g P_{high}$
ψ = purge flow, $v(purge)/v(prod)$
Ω = pressure ratio, P_{low}/P_{high}

Superscripts and subscripts

$*$ = equilibrium value
a = adsorbent
c = catalyst
g = gas phase
sat = saturation
i = component (A,B,C,D)
j = reaction (1,2)
ads = adsorption step
depres = depressurization step
high = upper pressure
low = upper pressure
pres = pressurization step
purge = purge inlet stream step

Arguments

exh = exhaust stream at P_{low}
prod = product stream at P_{high}
feed = feed stream
purge = purge inlet stream
PSR = pressure-swing reactor
PFR = plug-flow reactor
PSA = pressure-swing adsorber

Literature Cited

Alpay, E., "Rapid Pressure Swing Adsorption Processes," PhD Thesis, Univ. of Cambridge, Cambridge, England (1992).
Anand, M., S. Sircar, and B. T. Carvill, "Process for Operating Equilibrium Controlled Reactions," European Patent No. EP 0 737 648 (1996).
Carvill, B. T., J. R. Hufton, M. Amand, and S. Sircar, "Sorption-Enhanced Reaction Process," *AIChE J.*, **42**, 2765 (1996).
Chen, P., and R. T. Yang, "Bulk Gas Separation by Pressure Swing Adsorption," *Ind. Eng. Chem. Fundam.*, **25**, 758 (1986).
Derrien, M. L., "Selective Hydrogenation Applied to the Refining of Petrochemical Raw Materials Produced by Steam Cracking," *Stud. Surf. Sci. Catal.*, **27**, 613 (1986).
Farooq, S., D. Ruthven, and H. A. Boniface, "Numerical Simulation of a Pressure Swing Adsorption Oxygen Unit," *Chem. Eng. Sci.*, **44**, 2809 (1989).
Gaskell, P., and A. C. Lau, "Curvature-Compensated Convective Transport: SMART, A New Boundedness-Preserving Transport Algorithm," *Int. J. Numer. Methods Fluids*, **8**, 617 (1988).
Goto, S., T. Tagawa, and T. Oomiya, "Dehydrogenation of Cyclohexane in a PSA Reactor Using Hydrogen Storage Alloy," *Kagaku Kogaku Ronbunshu*, **19**, 978 (1993).
Han, C., and D. Harrison, "Simultaneous Shift Reaction and Carbon Dioxide Separation for the Direct Production of Hydrogen," *Chem. Eng. Sci.*, **49**, 5875 (1994).
Hufton, J. R., S. Mayorga, and S. Sircar, "Sorption-Enhanced Reaction Process for Hydrogen Production," *AIChE J.*, **45**, 248 (1999).
Kneabel, K., and E. Cussler, "A Novel Pressure Swing Adsorption System for Ammonia Synthesis," *Fundamentals of Adsorption: Proceedings of the Fifth International Conference on Fundamentals of Adsorption*, M. D. LeVan, ed., Kluwer, Boston, p. 457 (1996).
Kodde, A. J., and A. Bliek, "Selectivity Enhancement in Consecutive Reactions Using the Pressure Swing Reactor," *Stud. Surf. Sci. Catal.*, **109**, 419 (1997).
LaCava, A. I., A. I. Shirley, and R. Ramachandran, "How to Specify Pressure-Swing Adsorption Units," *Chem. Eng.*, **105**, 110 (1998).
Liden, G., and L. Wamling, "Periodic Operation of a Tubular Reactor: A Simulation Study of Consecutive Reactions in a Chromatographic Reactor," *Chem. Eng. J.*, **40**, 31 (1989).
Ruthven, D., *Principles of Adsorption and Adsorption Processes*, Wiley, New York (1984).
Ruthven, D., S. Farooq, and K. Kneabel, *Pressure Swing Adsorption*, VCH, New York (1994).
Sheikh, J., L. Kershenbaum, and E. Alpay, "Analytical Basis for Separation Enhanced Reaction in Continuous Flow Processes," *Chem. Eng. Sci.*, **53**, 2933 (1998).
Silva, J., and A. E. Rodriques, "Separation of *n*/iso-Paraffins Mixtures by Pressure Swing Adsorption," *Sep. Purif. Technol.*, **13**, 195 (1998).
Skarstrom, C., "Method and Apparatus for Fractionating Gaseous Mixtures by Adsorption," U.S. Patent No. 2,944,627 (1960).
Vaporciyan, G. G., and R. H. Kadlec, "Equilibrium-Limited Periodic Separating Reactors," *AIChE J.*, **33**, 1334 (1987).
Vaporciyan, G. G., and R. H. Kadlec, "Periodic Separating Reactors: Experiments and Theory," *AIChE J.*, **35**, 831 (1989).
Yang, J., C.-H. Lee, and Y.-W. Chang, "Separation of Hydrogen Mixture by a Two-Bed Pressure Swing Adsorption Process Using Zeolite 5A," *Ind. Eng. Chem. Res.*, **36**, 2789 (1997).
Yang, R. T., *Gas Separation by Adsorption Processes*, Butterworths, Stoneham, MA (1987).
Yongsunthon, I., and E. Alpay, "Design and Optimization of Temperature Cycled Adsorptive Reactors," *Comput. Chem. Eng.*, **22**, S733 (1998).
Yongsunthon, I., and E. Alpay, "Design of Periodic Adsorptive Reactors for the Optimal Integration of Reaction, Separation and Heat Exchange," *Chem. Eng. Sci.*, **54**, 2647 (1999).

Manuscript received Oct. 28, 1999, and revision received May 4, 2000.